

Statistics of PMD-Induced Power Fading for Intensity-Modulated Double-Sideband and Single-Sideband Microwave and Millimeter-Wave Signals

Olaf H. Adamczyk, *Student Member, IEEE*, Asaf B. Sahin, *Member, IEEE*, Qian Yu, *Member, IEEE*, Sanggeon Lee, *Student Member, IEEE*, and Alan E. Willner, *Senior Member, IEEE*

Abstract—Polarization-mode dispersion (PMD) can severely degrade the performance of millimeter-wave fiber-optic links by inducing a power fading penalty of the received signal that is dependent on the subcarrier frequency and accumulated PMD along the fiber. We experimentally investigate the statistics of PMD-induced power fading as a function of the differential group delay (DGD) for intensity-modulated double- and single-sideband subcarrier-multiplexed signals in the absence of chromatic dispersion. We find a similar susceptibility to PMD-induced power fading for both modulation formats with a subcarrier frequency of 7 GHz using a PMD emulator with a Maxwellian distribution of DGD (average DGD ~ 40 ps). A significant improvement in the worst case power fading penalty (~ 20 dB) is achieved by using an electronically controlled polarization controller in combination with a single section of polarization maintaining fiber in a dynamic first-order PMD compensator. Furthermore, the results of numerical Monte Carlo simulations support the measured data and show the scalability of PMD-induced power fading for subcarrier-multiplexed signals in the microwave and millimeter-wave region.

Index Terms—Double-sideband modulation, microwave photonics, optical fiber communication, PMD emulator, polarization-mode dispersion, power fading, single-sideband modulation, subcarrier multiplexing.

I. INTRODUCTION

POLARIZATION-MODE dispersion (PMD) is one of the critical challenges in next-generation millimeter-wave fiber links after the successful mitigation of chromatic dispersion effects, by inducing a severe power fading penalty resulting in a potential loss of the recovered signal. The cause for PMD is the unintentional circular asymmetry of optical fiber due to noncircular waveguide geometry or asymmetrical stress around

the fiber core. In an ideal symmetrical fiber, the state-of-polarization (SOP) of an optical wave can be represented as the superposition of two indistinguishable orthogonally polarized modes with the same propagation constants. However, the loss of circular symmetry in real fibers gives rise to two distinct orthogonally polarized modes with different propagation constants causing a difference in the group velocities [1]. This differential group velocity can be described by the differential group delay (DGD), i.e., first-order PMD, between the two orthogonal principal-states-of-polarization (PSPs) of the fiber. Due to random variations in the perturbations along the fiber span, the average DGD accumulates in a random fashion with a square-root of transmission length dependence and a Maxwellian probability distribution [2]–[4]. Furthermore, the perturbations vary over time due to temperature and other environmental changes causing a random fluctuation of PMD along the fiber link [5]. Although present-day fibers have PMD values ~ 0.1 ps/km $^{1/2}$, much of the fiber installed throughout the 1980's has PMD values ranging from 1 to as high as 10 ps/km $^{1/2}$. Therefore, the PMD characteristics of short spans of legacy fiber in an optical network can cause a negative effect in system performance by inducing a stochastic and dynamically changing degradation of high-speed digital baseband data channels [6], [7]. Transmission of analog and digital subcarrier-multiplexed (SCM) signals over fiber will also be severely affected by PMD [8], although its statistical impact on SCM signals has not yet been investigated. Therefore, it is imperative to examine the fading characteristics for SCM signals using a realistic PMD source that closely approximates the statistical nature of PMD in single-mode fiber.

The DGD between the fast and slow PSP of an optical sideband in a SCM signal causes a phase difference in the corresponding received subcarrier signals in the photodetector, as shown in Fig. 1. Superposition of the photocurrents may lead to serious power fading of the recovered subcarrier signal due to destructive interference that is a function of subcarrier frequency, accumulated DGD, and optical power splitting ratio between the PSPs [9]. The PMD-induced fading penalty in a microwave fiber link is essentially dependent on the subcarrier frequency (\gg GHz), which can be similar to the bit rates of high-speed optical baseband transmission systems, and not the data rate of the SCM signal itself ($<$ Gb/s). Such an optical

Manuscript received December 12, 2000; revised June 5, 2001.

O. H. Adamczyk was with the Department of Electrical Engineering, University of Southern California, Los Angeles, CA 90089-2565 USA. He is now with the Multilink Technology Corporation, Santa Monica, CA 90405 USA (e-mail: oadamczyk@mltc.com).

A. B. Sahin, Q. Yu, and A. E. Willner are with the Department of Electrical Engineering, University of Southern California, Los Angeles, CA 90089-2565 USA.

S. Lee was with the Department of Electrical Engineering, University of Southern California, Los Angeles, CA 90089-2565 USA. He is now with Phaethon Communications Inc., Fremont, CA 94538 USA.

Publisher Item Identifier S 0018-9480(01)08718-X.

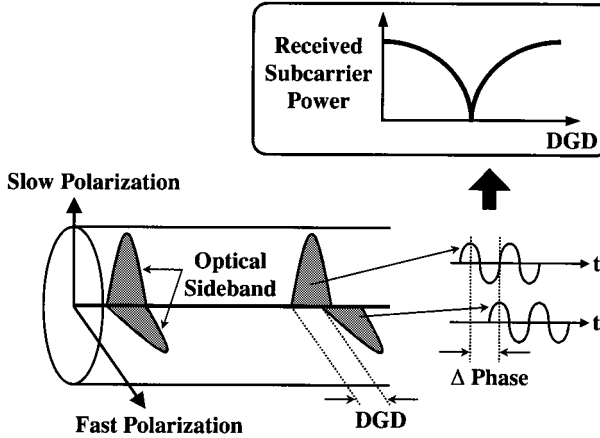


Fig. 1. PMD induces a DGD between the fast and slow PSP of an optical sideband, causing a phase difference in the corresponding received subcarrier signals in the photodetector. Superposition of the photocurrents may lead to serious power fading of the recovered subcarrier signal.

link may accumulate PMD values of ~ 10 ps over a 100-km distance leading to a significant fading penalty for the transmitted millimeter-wave signals. Furthermore, higher order PMD, such as polarization-dependent chromatic dispersion and depolarization effects, can cause additional distortion and degradation of the transmitted signal [10], [11].

PMD-induced power fading is similar to the fading that occurs in conventional intensity-modulated double-sideband (DSB) systems due to chromatic dispersion [12], [13]. Although it has been shown that single-sideband (SSB) transmission is relatively immune to chromatic dispersion [14], it is unclear whether SSB intensity modulation is also beneficial in reducing PMD-induced fading.

In this paper, we experimentally and numerically investigate the statistics of PMD-induced power fading as a function of DGD for DSB-SCM and SSB-SCM signals using a realistic PMD source. Section II describes the experimental setup including the 15-section PMD emulator to conduct the measurements. In Section III, we present the results of our measurements for DSB and SSB intensity modulated subcarrier signals under high PMD conditions (DGD ~ 40 ps) with and without first-order compensation. Results from numerical Monte Carlo simulations for both modulation formats in the microwave and millimeter-wave region are shown in Section IV.

II. EXPERIMENTAL SETUP

It is critical to accurately emulate the PMD characteristics of real embedded fiber systems to ensure a correct assessment of the PMD impairments for the DSB-SCM and SSB-SCM modulation formats. One important characteristic of such an emulator is its ability to approximate the Maxwellian distribution of DGD. Fig. 2(a) shows the PMD emulator composed of 15 sections of polarization-maintaining (PM) fiber with nine polarization controllers (PCs) distributed between the sections to realize different polarization coupling and, therefore, enable a close emulation of the Maxwellian distribution of DGD [15]. The length of the PM fiber sections are chosen randomly, with an average of ~ 7 m and a 20% Gaussian deviation, to generate

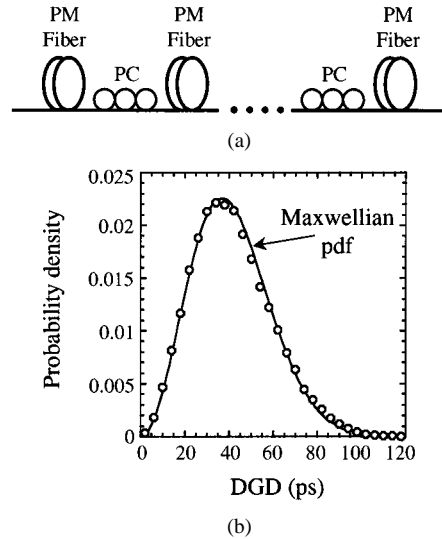


Fig. 2. (a) The PMD emulator consists of 15 sections of PM fiber of varying length with polarization controllers distributed between them. (b) Measured DGD pdf for the 15-section emulator. Solid line shows ideal Maxwellian distribution.

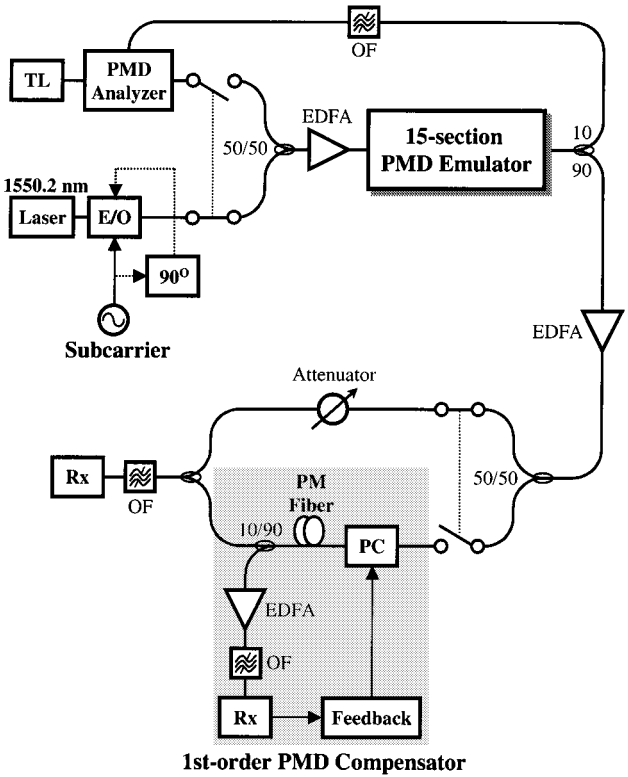


Fig. 3. Experimental setup to evaluate the statistics of PMD-induced power fading. (TL: tunable laser; 90° : phase shifter; PC: polarization controller; OF: optical filter; Rx: receiver).

an average PMD of ~ 40 ps [16]. The measured DGD probability density function (pdf) for the 15-section emulator is shown in Fig. 2(b). A good agreement with the Maxwellian DGD distribution can be observed by changing the polarization coupling between the PM fiber sections in a random fashion.

Fig. 3 shows the experimental setup used to compare DSB and SSB modulation formats under high PMD conditions. Besides conventional DSB intensity modulation using an external

single-electrode Mach-Zehnder (MZ) modulator, SSB modulation is achieved by employing a dual-electrode MZ modulator and driving the second input with a 90° phase-shifted copy of the subcarrier signal input to the first electrode [17]. Both external modulators are biased at the quadrature point. The input signal to the following PMD emulator can be selected between the modulated signal and the PMD analyzer output to either induce PMD onto the subcarrier signal or to measure the actual DGD value of the PMD emulator, respectively. The PMD analyzer uses a tunable laser in the same wavelength region as the subcarrier modulated light (1550.2 nm) to determine the DGD value of each emulator state. Different emulator states are generated by randomly changing the polarization coupling inside the emulator using the distributed PCs.

The subcarrier signals can be detected directly without any compensation or after traversing through a first-order PMD compensator by selecting the corresponding optical path before the receiver. The dynamic first-order PMD compensator consists of an electronically controlled PC followed by a 24-m-long section of PM fiber with a DGD of ~ 42 ps [18]. Some of the light is detected after the PM fiber to generate a feedback signal by mixing the received subcarrier signal with itself. The electronically controlled PC maximizes the feedback signal, which is proportional to the received subcarrier power, by optimizing the polarization coupling into the PM fiber. The received compensated and uncompensated subcarrier power is measured for each emulator state using equal optical power levels at the photo detector. Note that there is no chromatic dispersion present in the setup.

III. EXPERIMENTAL RESULTS

We measured the received subcarrier power and the corresponding DGD values for 350 independent polarization samples by randomly changing the polarization coupling inside the PMD emulator for DSB and SSB intensity modulation using a 7-GHz subcarrier. Fig. 4(a) shows the normalized received subcarrier power versus DGD for DSB and SSB formats without compensation. The solid line in each figure plots the maximum theoretical fading curve for a 7-GHz subcarrier for equal polarization coupling into the PSPs for first-order PMD (i.e., DGD) only. In this case, the received subcarrier power is proportional to $\cos^2(\pi \cdot f_{\text{sub}} \cdot \text{DGD})$, with f_{sub} being the subcarrier frequency [19]. For an infinite number of samples, the data points of the measured subcarrier power would fill out the area inside the theoretical fading curve with only DGD present due to the random polarization coupling into the PSP's. The combination of DGD and higher order PMD can lead to data points outside the theoretical fading curve, exhibiting significant fading penalties (>20 dB). This clearly indicates the importance of using a realistic PMD source with a Maxwellian DGD distribution and higher-order PMD effects. The DSB and SSB intensity modulated signals exhibit a similar sensitivity to PMD-induced power fading. Unlike for the case of chromatic dispersion, SSB modulation does not avoid a fading penalty since the PMD effects apply directly to the single optical sideband which is split into the PSPs, causing serious power fading even if only one optical

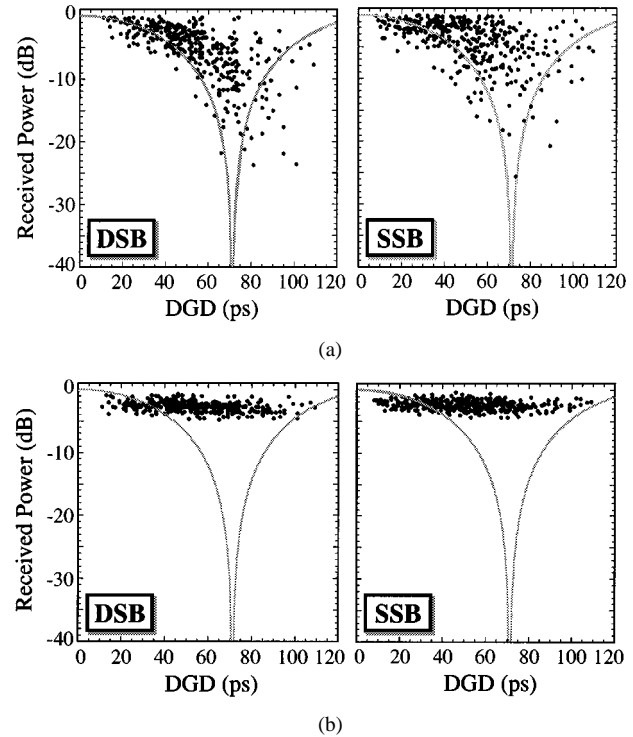


Fig. 4. Normalized measured subcarrier power versus DGD for 350 independent polarization samples using DSB and SSB intensity-modulated subcarrier signals ($f_{\text{sub}} = 7$ GHz). (a) Without compensation. (b) With dynamic first-order PMD compensation. Solid line corresponds to the theoretical fading curve for equal polarization coupling into the PSP for first-order PMD (i.e., DGD).

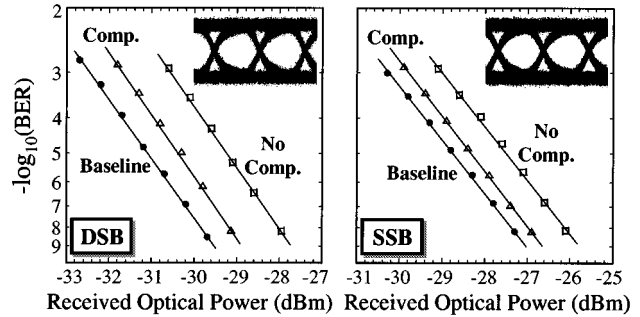


Fig. 5. Measured BER versus received optical power for 155-Mb/s DSB-SCM-BPSK and SSB-SCM-BPSK signals at 7 GHz with and without first-order compensation. Measured DGD value of the emulator state is ~ 40 ps for both modulation formats. The insets show a recovered eye diagram at $\text{BER} = 10^{-9}$ for both formats with first-order PMD compensation.

sideband is present. Using the dynamic first-order compensation technique, the worst case fading penalty can be reduced by ~ 20 dB to less than 5 dB for both modulation formats, as shown in Fig. 4(b).

A 155-Mb/s binary data channel is up-converted to a 7-GHz microwave subcarrier in order to generate a binary-phase-shift-keyed (BPSK) SCM signal. The SCM-BPSK data is optically transmitted using DSB and SSB intensity modulation. The DGD value of the PMD emulator is adjusted to approximately 40 ps to measure the performance of both modulation formats with and without first-order compensation. Fig. 5 shows the measured bit error rate (BER) versus the received optical power for the DSB-SCM-BPSK and SSB-SCM-BPSK signals. The

baseline is obtained without the PMD emulator. DSB modulation exhibits a better baseline sensitivity by ~ 2.5 dB due to the different setup and modulators used for the two modulation schemes. The power penalty without compensation is >1.5 dB for both formats, and improves to <0.5 dB with first-order compensation. Note that the PMD emulator is adjusted to be able to achieve a BER of 10^{-9} without first-order compensation. Variations in the polarization coupling inside the emulator may lead to a large power penalty (without compensation) resulting in an error floor for the BER measurements.

IV. NUMERICAL RESULTS

Numerical Monte Carlo simulations using Maxwellian PMD statistics were performed for comparison with the experimental data. The system model follows the experimental setup with DSB and SSB intensity-modulated subcarrier signals. The PMD emulator is modeled as a concatenation of 50 DGD segments of unequal length, each having a random DGD value with a Maxwellian distribution and a random PSP orientation (uniform distribution on the Poincaré sphere) [20]. The PMD vector grows in a random-walk-like process, therefore generating Maxwellian PMD statistics including all-order PMD effects. Fiber chromatic dispersion and nonlinearities are omitted. Exact first-order compensation completely eliminates the DGD in the PMD vector generated in the emulator, thus only higher order PMD is present before detection. The simulations are performed for 10 000 independent polarization samples for each modulation format, with and without first-order compensation.

Fig. 6 shows the simulation results for PMD-induced power fading versus DGD for a DSB and SSB intensity modulated 7-GHz subcarrier signal: (a) without compensation and (b) with first-order compensation. The average DGD of the modeled fiber link is set to 40 ps. The simulations exhibit a qualitatively comparable performance to the measured data for both formats with and without compensation. The 100 worst case samples for both formats, i.e., 1% of the samples, experience >14 dB of PMD-induced power fading without compensation and >4 dB with first-order compensation. The power variances for 0.1% of the data points are ~ 24 dB without and ~ 7.5 dB with compensation for both formats (i.e., power penalty for the ten worst case samples is greater than the power variance). The larger maximum fading penalty compared to the measurements may come from the limited number of samples taken in the experiment.

To show the scalability of the PMD-induced power fading in the frequency domain, simulations were performed for 30-GHz DSB and SSB modulated millimeter-wave signals. The average DGD of the modeled fiber link with Maxwellian PMD statistics is reduced to 10 ps. The simulation results for the 30-GHz DSB and SSB signals are shown in Fig. 7(a) without compensation and in Fig. 7(b) with ideal first-order compensation. A similar response to the PMD-induced fading can be seen compared to the 7-GHz subcarrier signals. In summary, an average DGD value of $<20\%$ of the period of the subcarrier signals (<30 ps

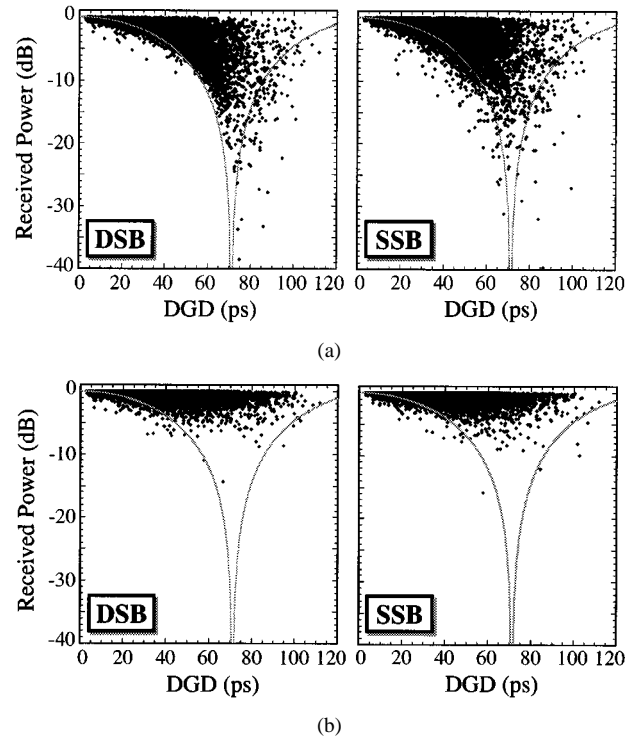


Fig. 6. Numerical simulations of the received subcarrier power versus DGD for 10 000 independent polarization samples using DSB and SSB intensity modulated subcarrier signal ($f_{\text{sub}} = 7$ GHz). (a) Without compensation. (b) With dynamic first-order PMD compensation. Solid line corresponds to the theoretical fading curve for equal polarization coupling into the PSP for first-order PMD.

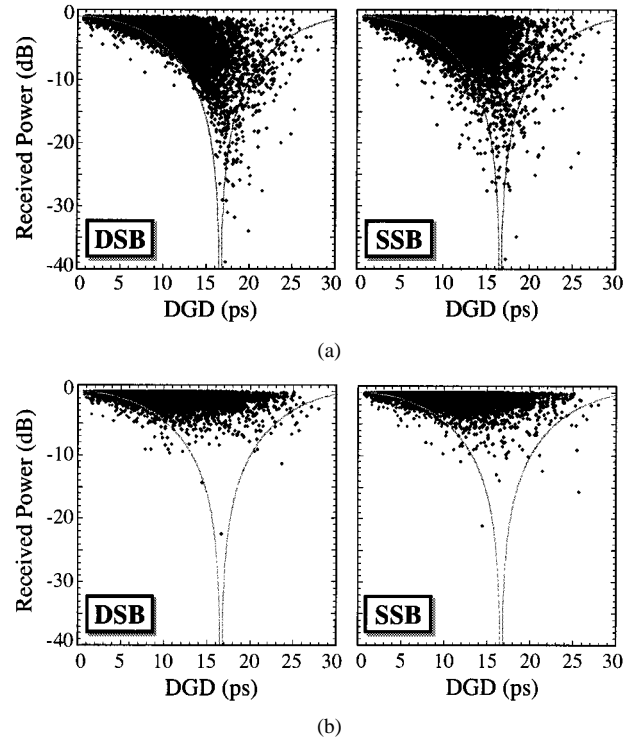


Fig. 7. Numerical simulations of the received subcarrier power versus DGD for 10 000 independent polarization samples using DSB and SSB intensity modulated subcarrier signal ($f_{\text{sub}} = 30$ GHz). (a) Without compensation. (b) With dynamic first-order PMD compensation.

and <7 ps for 7 and 30 GHz, respectively), can lead to a significant power fading penalty and severely degrade system performance in a millimeter-wave fiber-optic link.

V. CONCLUSION

We investigated the statistics of PMD-induced power fading for DSB and SSB intensity modulated microwave and millimeter-wave signals. We measured a comparable sensitivity to PMD-induced power fading for a 7-GHz subcarrier signal for both modulation formats using a PMD emulator composed of 15 sections of PM fiber with polarization controllers distributed between them (average DGD ~ 40 ps). Such an emulator produces an almost ideal Maxwellian distribution of DGD to closely simulate the PMD characteristics of real embedded fiber links. A dynamic first-order PMD compensator consisting of an electronic controlled polarization controller and a single section of PM fiber improved the worst case fading penalty by ~ 20 dB. Numerical Monte Carlo simulations of 10 000 independent polarization samples for a 7-GHz DSB and SSB intensity modulated subcarrier signal supported the experimental data (average DGD = 40 ps). Furthermore, simulation results for a 30-GHz millimeter-wave subcarrier with the average DGD in the fiber span reduced to 10 ps indicated the scalability of PMD-induced power fading to higher frequencies.

ACKNOWLEDGMENT

The authors would like to thank R. Khosravani and Y. Xie for their support with the experimental setup of the PMD emulator.

REFERENCES

- [1] J. Sakai and T. Kimura, "Birefringence and polarization characteristics of single-mode optical fibers under elastic deformations," *IEEE J. Quantum Electron.*, vol. QE-17, pp. 1041–1051, July 1981.
- [2] G. J. Foschini and C. D. Poole, "Statistical theory of polarization dispersion in single mode fiber," *J. Lightwave Technol.*, vol. 9, pp. 1439–1456, Nov. 1991.
- [3] F. Curti, B. Daino, G. de Marchis, and F. Matera, "Statistical treatment of the evolution of the principal states of polarization in single-mode fiber," *J. Lightwave Technol.*, vol. 8, pp. 1162–1166, Aug. 1990.
- [4] N. Gisin, R. Passy, J. C. Bishoff, and B. Perny, "Experimental investigations of the statistical properties of polarization mode dispersion in single mode fibers," *IEEE Photon. Technol. Lett.*, vol. 5, pp. 819–821, July 1993.
- [5] B. W. Hakki, "Polarization mode dispersion in a single mode fiber," *J. Lightwave Technol.*, vol. 14, pp. 2202–2208, Oct. 1996.
- [6] H. Bülow, "Polarization mode dispersion (PMD) sensitivity of a 10 Gbit/s transmission system," in *Proc. Eur. Opt. Commun. Conf.*, Sept. 1996, TuD.3.6, pp. 2.211–2.214.
- [7] S. Lee, Y. Xie, O. H. Adamczyk, and A. E. Willner, "Penalty distribution comparison for different data formats under high PMD values," in *Proc. Eur. Opt. Commun. Conf.*, Sept. 2000, 5.2.2, pp. 93–94.
- [8] C. D. Poole and T. E. Darcie, "Distortion related to polarization-mode-dispersion in analog lightwave systems," *J. Lightwave Technol.*, vol. 11, pp. 1749–1759, Nov. 1993.
- [9] R. Hofstetter, H. Schmuck, and R. Heidemann, "Dispersion effects in optical millimeter-wave systems using self-heterodyne method for transport and generation," *IEEE Trans. Microwave Theory Tech.*, vol. 43, pp. 2263–2269, Sept. 1995.
- [10] R. M. Jopson, L. E. Nelson, H. Kogelnik, and G. J. Foschini, "Polarization mode dispersion beyond first order," in *IEEE LEOS 12th Annu. Meeting Tech. Dig.*, 1999, pp. 149–150.
- [11] P. Ciprut, B. Gisin, N. Gisin, R. Passy, J. P. von der Weid, F. Prieto, and C. W. Zimmer, "Second-order polarization mode dispersion: Impact on analog and digital transmissions," *J. Lightwave Technol.*, vol. 16, pp. 757–771, May 1998.
- [12] H. Schmuck, "Comparison of optical millimeter-wave system concepts with regard to chromatic dispersion," *Electron. Lett.*, vol. 31, pp. 1848–1849, Oct. 1995.
- [13] U. Gliese, S. Nørskov, and T. N. Nielsen, "Chromatic dispersion in fiber-optic microwave and millimeter-wave links," *IEEE Trans. Microwave Theory Tech.*, vol. 44, pp. 1716–1724, Oct. 1996.
- [14] K. Yonenaga and N. Takachio, "A fiber chromatic dispersion technique with an optical SSB transmission in optical homodyne detection systems," *IEEE Photon. Technol. Lett.*, vol. 5, pp. 949–951, Aug. 1993.
- [15] I. T. Lima, R. Khosravani, P. Ebrahimi, E. Ibragimov, A. E. Willner, and C. R. Menyuk, "Polarization mode dispersion emulator," in *Opt. Fiber Commun. Conf. Tech. Dig.*, Mar. 2000, ThB4, pp. 31–33.
- [16] C. H. Prola, Jr., J. A. Pereira da Silva, A. O. Dal Forno, R. Passy, J. P. von der Weid, and N. Gisin, "PMD emulators and signal distortion in 2.48-Gb/s IM-DD lightwave systems," *IEEE Photon. Technol. Lett.*, vol. 9, pp. 8142–8144, June 1997.
- [17] G. H. Smith, D. Novak, and Z. Ahmed, "Technique for optical SSB generation to overcome dispersion penalties in fiber-radio systems," *Electron. Lett.*, vol. 33, pp. 74–75, Jan. 1997.
- [18] T. Takahashi, T. Imai, and M. Aiki, "Automatic compensation technique for timewise fluctuating polarization mode dispersion in in-line amplifier systems," *Electron. Lett.*, vol. 30, pp. 348–349, Feb. 1994.
- [19] H. Schmuck, "Effect of polarization-mode-dispersion in fiber-optic millimeter-wave systems," *Electron. Lett.*, vol. 30, pp. 1503–1504, Sept. 1994.
- [20] Q. Yu, L. Yan, S. Lee, Y. Xie, M. Hauer, Z. Pan, and A. E. Willner, "Enhanced higher-order PMD compensation using a variable time delay between polarizations," in *Proc. Eur. Opt. Commun. Conf.*, Sept. 2000, 4.2.7, pp. 47–48.

Olaf H. Adamczyk (S'96) received the Dipl.-Ing. degree in electrical engineering from the Ruhr University Bochum, Bochum, Germany, in 1994, and the M.S. and Ph.D. degrees in electrical engineering from the University of Southern California (USC), Los Angeles, in 1997 and 2001, respectively.

From 1994 to 1995, he was a Research Associate at the High Speed Technology Laboratory, USC. In 2001, he became a Senior Design Engineer with Multilink Technology Corporation, Santa Monica, CA. His research interests include high-speed electronic circuit design and device characterization, optical-fiber communication systems, microwave and millimeter-wave fiber-optic links, and high-capacity wavelength division multiplexed (WDM) transmission systems.

Asaf B. Sahin (M'99) received the B.S. degree in electrical and electronics engineering from the Middle East Technical University, Ankara, Turkey, in 1996, the M.S. degree from the University of Southern California (USC), Los Angeles, in 1998, and is currently working toward the Ph.D. degree in electrical engineering at USC.

His field of study is optical communication systems, especially concentrating on microwave signal transmission over fiber-optical links. He has authored several publications in that field.

Mr. Sahin is a member of the IEEE Lasers and Electro-Optics Society, the IEEE Communications Society, and the Optical Society of America.

Qian Yu (S'96–M'99) was born in Shanghai, China, in 1973. He received the B.S. and Ph.D. degrees in electronics engineering from the Tsinghua University, Beijing, China, in 1994 and 1999, respectively.

He is currently a Post-Doctoral Research Associate in the Department of Electrical Engineering Systems, University of Southern California, Los Angeles. He has authored or co-authored 20 refereed publications. His research has been focused on fiber-optic communication systems, particularly fiber nonlinearities and polarization effects.

Sanggeon Lee (S'97) was born in Pusan, Korea, in 1970. He received the B.S. degree in nuclear engineering from the Seoul National University, Seoul, Korea, in 1992, and the M.A. and Ph.D. degrees in physics from the University of Southern California, Los Angeles, in 1998 and 2000, respectively.

In 2000, he joined Phaethon Communications Inc., Fremont, CA. His main areas of interest include characterization and compensation of polarization mode dispersion for high-speed optical transmission systems, high-speed and high-capacity WDM systems, dispersion compensation techniques, and fiber gratings and their applications.

Alan E. Willner (S'87–M'88–SM'93) received the Ph.D. degree in electrical engineering from Columbia University, New York, NY, in 1988.

He was a Post-Doctoral Member of the Technical Staff at AT&T Bell Laboratories, Crawford Hill, NJ, and a Member of Technical Staff at Bellcore. He is currently a Professor of electrical engineering systems at the University of Southern California (USC), Los Angeles. He is also the Associate Director for the USC Center for Photonics Technology and is an Associate Director for Student Affairs for the National Science Foundation (NSF) Engineering Research Center in Multimedia. He has authored or co-authored 285 publications, including one book and four book chapters. His research is in the area of optical-fiber communication systems, WDM, optical amplification, optical networks, optical switching, and optical interconnections.

Prof. Willner is a Fellow of the Optical Society of America (OSA) and the Semiconductor Research Corporation. His professional activities include vice-president for Technical Affairs for the IEEE Lasers and Electro-Optics Society (IEEE LEOS), elected member of the Board of Governors for the IEEE LEOS, chair-elect of the Science and Engineering Council as well as photonics division chair of the OSA, general chair of the IEEE LEOS Annual Meeting, program co-chair of the OSA Annual Meeting, program co-chair of the Conference on Lasers and Electro-Optics (CLEO), general co-chair of the OSA Optical Amplifier Conference, general co-chair of the IEEE LEOS Topical Meeting on Broadband Optical Networks, Steering Committee and Technical Committee member of the Conference on Optical Fiber Communications (OFC), Technical Program Committee member of the European Conference on Optical Communications, chair of the Optical Communications and Optical Networks IEEE LEOS Technical Committees, vice-chair of the Optical Communications Group of the OSA's Technical Council, and Technical Program Committee member of the IEEE Microwave Photonics Conference. His editorial positions have included editor-in-chief of the JOURNAL OF LIGHTWAVE TECHNOLOGY, guest editor of the IEEE JOURNAL OF SELECTED TOPICS IN QUANTUM ELECTRONICS and IEEE JOURNAL ON SELECTED AREAS IN COMMUNICATIONS, and guest editor for the IEEE JOURNAL OF QUANTUM ELECTRONICS. He was the recipient of the Presidential Faculty Fellows Award from the White House, the David and Lucile Packard Foundation Fellowship, the National Science Foundation (NSF) Young Investigator Award, the Fulbright Foundation Senior Scholar Fellowship, the IEEE LEOS Distinguished Lecturer Award, and the USC/Northrop Outstanding Junior Engineering Faculty Research Award.